Mechanistic insights into sulfur rich oil formation, relevant to geological carbon storage routes. A study using APPI-P FTICR-MS(/MS) analysis

Renzo C. Silva*, Calista Yim, Jagoš R. Radović, Melisa Brown, Priyanthi Weerawardhena, Haiping Huang, Lloyd R. Snowdon, Thomas B.P. Oldenburg, Steve R. Larter

PRG, Department of Geoscience, University of Calgary, 2500 University Drive NW, T2N 1N4, Calgary, AB, Canada.

Abstract

Sulfur incorporation into sedimentary organic matter has a key role in carbon preservation in the geosphere. Such processes can inform strategies for human timescale carbon storage to mitigate climate change impacts and thus more detailed knowledge of sulfur incorporation into biomass species is needed. Until recently, detailed chemical characterization of sulfurized organic matter was only possible by analyzing individual building blocks obtained after desulfurization reactions. In this study, Fourier transform ion cyclotron resonance mass spectrometry (FTICR-MS), with atmospheric pressure photoionization in positive ion mode (APPI-P) was used to investigate the chemical composition of sulfur rich crude oils and to obtain mechanistic insights into the sulfur incorporation reactions happening during early diagenesis. Contrary to the current body of knowledge, APPI-P FTICR-MS data show that sulfurized lipids (with up to 6 sulfur atoms) occur as free molecules in these oils, rather than within a macromolecular network linked by (poly)sulfide bridges. In contrast to Peace River (Canada) oils, the thermally immature Rozel Point (USA) and Jianghan Basin (China) oils show a carbon number preference in sulfurized species resembling biogenic precursor molecules, which highlights the importance of S-bound molecules as geochemical proxies for early diagenetic processes. This study indicates that sulfur incorporation reactions involve the formation of S-cyclic structures in which the double bond equivalent is $\geq$ the number of S atoms, which can then aromatize to thiophenes depending on the thermal stress level they experience. FTICR-MS/MS experiments suggest the occurrence of intermolecular sulfur incorporation reactions, but only as a mechanism secondary to intramolecular sulfur addition. The FTICR-MS/MS fragmentation studies also indicate the aliphatic nature of class S_1 species and sulfurized alkenones, the preference of cycle-forming sulfur incorporation in steroid structures, and the occurrence, to a minor extent, of thiol/thioether

groups. Knowledge of organic sulfur molecule formation informs routes for carbon dioxide removal technologies which could sequester carbon in the geosphere and/or hydrosphere in the form of recalcitrant organic species.

1. Introduction

Sulfur incorporation into sedimentary organic matter has a key role in carbon preservation in the geosphere, occurring on short geological timescales, not only on Earth but also possibly on Mars (Werne et al., 2004; Summons et al., 2011). The understanding of mechanisms and geochemical implications of sulfur incorporation reactions expanded greatly during the late 1980s and early 1990s (Orr and Sinninghe Damsté, 1990; Aizenshtat et al., 1995; Amrani, 2014), and given their relevant role in enabling an important carbon sink, there are still many active areas of research in the field. For example, there currently exists a heightened research interest to further understand carbon preservation mechanisms via sulfur incorporation (Raven et al., 2016; Pohlabeln et al., 2017) in the context of the global change and the need to keep the global temperature increase to <2 °C by the end of this century (IPCC, 2018).

Large scales of carbon removal are not unusual in natural systems. The global ocean has pools of organic carbon found in dissolved and particulate form in the water column, or deposited in the deep-sea sediments which are of similar magnitude to atmospheric carbon reservoirs (Houghton, 2007; Hansell et al., 2009; Jiao et al., 2010). Therefore, a better understanding of natural mechanisms for long term preservation of organic molecules in the geosphere can provide guidelines for the development of technologies that artificially enhance the removal of carbon from the atmosphere to ocean or subsurface reservoirs, in the form of biologically refractory organic species analogous to those already present naturally in the Earth.

During the early diagenesis, sulfurized organic compounds, commonly occurring in anoxic environments that are rich in reduced sulfur, would typically resemble their biological precursors. As the diagenesis progresses, extensive sulfurization reactions enable multi-point, intermolecular cross-linkage, eventually generating the macromolecular structures which are the building blocks of sulfur rich kerogen (type II-S) (Tegelaar et al., 1989; Vandenbroucke and Largeau, 2007). Sulfur rich macromolecular structures were also detected in thermally immature, sulfur rich oils (Sinninghe Damsté et al., 1987; Sinninghe Damsté et al., 1989; Orr and Sinninghe Damsté, 1990). However, the detailed chemical characterization of such compounds was only possible by analyzing individual building blocks after desulfurization reactions (Adam et al., 1992; Adam et al., 1993; Richnow et al., 1993). Since then, analytical technologies have greatly advanced. Ultrahigh resolution mass spectrometry, in particular the FTICR-MS (Fourier

transform ion cyclotron resonance mass spectrometry) technology, has enabled the identification of several thousand peaks in complex organic mixtures, revolutionizing the understanding of the petroleome (Marshall and Rodgers, 2008). In the field of organic geochemistry, such technical advances were translated into an unprecedented capability to probe the high molecular weight, polar compounds at a high level of detail, expanding the way biodegradation, thermal stress and other biogeochemical processes are understood (Oldenburg et al., 2014; Radović et al., 2015; Radović et al., 2016b; Oldenburg et al., 2017).

Investigations focused on the geochemical significance of sulfur species have also greatly benefited from ultrahigh resolution mass spectrometry applications. Hughey et al. (2004) analyzed two same sourced Smackover Formation oils of different levels of thermal maturity using ESI-N (electrospray ionization in negative ion mode) FTICR-MS, suggesting the removal of sulfur and oxygen compounds was promoted by thermal maturation. Similarly, Oldenburg et al. (2014) reported that the relative apparent abundances of all heteroatom-containing compound classes (nitrogen, oxygen, sulfur and mixed heteroatom species) detected in that study decreased systematically with increasing oil maturation levels. Walters et al. (2015) used both APPI-P (atmospheric pressure photoionization in positive-ion mode) and ESI-N FTICR-MS to probe sulfur compounds and oxygenated analogs present in samples from the Smackover Formation, revealing intermediates (classes O_x and SO_x) of thermochemical sulfate reduction (TSR) redox reactions. A similar approach detected the formation of TSR induced proto-solid bitumen, including highly condensed polynuclear aromatic and naphthenoaromatic species with up to three sulfur atoms (Walters et al., 2011). Lu et al. (2013) used ESI-P (electrospray ionization in positive-ion mode) FTICR-MS to investigate sulfur rich heavy oils from Bohai Bay Basin, reporting a wide range of sulfurized sedimentary steroids in addition to a complex distribution of sulfur and oxidized sulfur compounds. Based on a similar approach, Lu et al. (2014) detected high levels of alkylcyclothioethers within Jianghan Basin oils. More recently, Liu et al. (2018) reported an in-depth investigation of polar sulfur compounds in immature crude oils from the Jianghan Basin via ESI-N and ESI-P FTICR-MS and showed that the detected S-bearing species are mostly cyclic, originating from intramolecular sulfurization of functionalized precursors during early diagenesis. The authors inferred that the extent of intramolecular sulfurization is based on the number of reactive functional groups in the precursor molecule.

Expanding on these findings, the present study investigates the compounds present in a suite of sulfur rich oils and their fractions via APPI-P FTICR-MS and APPI-P FTICR-MS/MS experiments. Extended compositional information of high molecular weight, sulfur bearing molecules that could not be detected in earlier GC based studies is presented and critically discussed based on the current understanding of sulfur incorporation into organic matter. This paper aims to gather new insights from sulfur rich oil molecular composition to probe the mechanisms of sulfur incorporation into sedimentary organic matter, which could possibly be leveraged for the development of carbon dioxide removal (CDR) technologies.

2. Materials and methods

2.1. Sample set description

Five sulfur rich oils from different basins were selected in this study: (a) three high maturity, highly biodegraded oils from the Peace River area, Canada; (b) one immature oil from the Jianghan Basin, Eastern China; and (c) one immature oil from the Rozel Point, Utah, USA (Table 1).

Rozel Point is an immature, sulfur-rich heavy oil generated from a hypersaline, lacustrine source rock of Miocene age (Meissner et al., 1984; ten Haven et al., 1988; Sinninghe Damsté et al., 1989). High concentrations of organic sulfur (up to 15 wt%) and the unique depositional environment that characterizes Rozel Point oil have motivated many studies of the origin and fate of organically bonded sulfur during early diagenesis, with implications for the understanding of Type II-S kerogen formation (Eglinton et al., 1994). The Jianghan Basin, located in eastern China, is comprised of five major tectonic units with the Qianjiang depression being the most significant structure since most oil production takes place in this region from the Eocene Qianjiang Formation (Philp and Zhaoan, 1987). Oils from the Qianjiang depression are sourced from the Qianjiang Formation and Xingouzui Formation, which were deposited in anoxic, sulfate reducing and saline lacustrine environments during the early Cretaceous to Paleogene (Carroll and Bohacs, 2001; Hou et al., 2017). Due to cycles of marine transgression and progradation activity, hot paleoclimate, and clastic sediment deposition from lacustrine systems, over 220 evaporitic layers interlaced with shales and sandstones formed the Jianghan Basin source rocks (Philp and Zhaoan, 1987; Peirong et al., 2008; Hou et al., 2017). The Qianjiang Formation is suspected to act as both the source rock and reservoir (Philp and Zhaoan, 1987; Huang and

Hinnov, 2014; Hou et al., 2017). Upper Qianjiang sections act as the oil reservoir while the deeper sections and Xingouzui Formation embody the source rock. Oils from the Qianjiang Formation typically exhibit a pronounced even/odd *n*-alkane predominance, low ratios of Pr/Ph and high ratios of gammacerane/hopane, indicating a highly anoxic, reducing and saline depositional environment (Philp and Zhaoan, 1987). The Peace River oil sands, located in northwestern Alberta, is one of three major bitumen deposits in that province. The Peace River area is comprised of two main groups, the Bullhead Group formed by the Cadomin and Gething formations, and the overlying Fort St. John Group which, in succession, comprises the Bluesky, Spirit River, Peace River and Shaftesbury formations. Peace River oil reservoirs, Bluesky, Gething and McMurray, are late Paleozoic to Mesozoic in age and are charged by Cretaceous oil source rocks (Adams et al., 2012). The reservoirs are supplied with a mixture of hydrocarbons expelled from multiple source rocks including the Nordegg Member of Fernie Formation, Gordondale Formation and Permian Doig Formation (Riediger, 1994; Adams et al., 2013). Manville Group reservoirs, Bluesky and Gething, may also be vertically charged by the Mississippian Exshaw-Banff formations where hydrocarbons migrated upwards to permeable Cretaceous sand units when erosion deteriorated the seal enforced by the Poker Chip shale (Allan and Creaney, 1991). Peace River bitumen, which exhibits high levels of biodegradation, such as those from the Bluesky Formation, are sourced by Exshaw - Banff source rock as these oils had a longer residence time in the reservoir. On the other hand, deposits in the western part of Peace River received more significant contributions from Gordondale source rock as these oils are higher in sulfur content, less mature and have greater API gravity (Adams et al., 2013).

2.2. Non-polar macromolecular fractions

The experimental procedure used to obtain the non-polar macromolecular fraction (NPMF) from Rozel Point and Jianghan oils was adapted from Adam et al. (1993). In brief, aliquots of the crude oils (~100 mg) were loaded on a silica gel (6.0 g, 220-440 mesh) column. The samples were washed with 50 mL of hexane and then eluted with 15 mL of hexane:diethyl ether (98:2), which yielded the NPMF orange-colored band that was collected, evaporated to dryness and submitted to APPI-P FTICR-MS analysis. NPFM was not produced from western Canadian oils indicating that the macromolecular fraction was not present in such mature and overmature oils.

2.3.Mass spectrometry

APPI-P is the ionization technique of choice for sulfur-rich sample analysis due to its enhanced ability to ionize sulfur compounds in complex organic mixtures without chemical derivatization nor special sample preparation strategies (Purcell et al., 2006; Oldenburg et al., 2014). Two primary ionization mechanisms are expected to occur in the APPI-P source: proton transfer, which generates even electron protonated ions depending on the proton affinity of the analyte; and the formation of an odd electron radical ion species (Raffaelli and Saba, 2003). Note that the thermospray conditions in APPI-P show negligible in-source thermal alteration of species (Bagag et al., 2008).

Even though it was demonstrated in previous studies that APPI-P FTICR-MS has some very rudimentary quantitation capabilities (Oldenburg et al., 2014), due to unassessed differences in ionization responses, intensities cannot be assumed to reflect the actual abundance of compounds present in the sample. Thus, quantitative aspects of compounds and compound classes are not considered herein; only relative intensities are discussed, based on monoisotopic peak intensities of assigned peaks (RMI, relative monoisotopic intensity). Also, structural discussions of detected species are only speculative, since FTICR-MS data provide unambiguous molecular formulas but cannot distinguish isomers.

Attempts to perform FTICR-MS/MS experiments in complex mixtures provide limited but potentially useful information. Targeted peaks may represent a dozen to potentially thousands of different isomers, as no prior chromatographic clean up was performed in these experiments. Therefore, the measured fragmentation patterns represent the conflation of the fragmentation patterns of all the isomers with the targeted molecular formula. The isolation window ($m/z \pm 0.4$) used in this study may contain 10+ peaks. Thus, only peaks with the highest intensity within their $m/z \pm 0.4$ spectral windows were selected for MS/MS experiments. To avoid interferences with fragments originating from other parent peaks within the $m/z \pm 0.4$ windows, detected peaks with more carbon or sulfur atoms than the parent ion were ignored. Peaks detected in MS/MS mode were assigned molecular formulae with assignment errors < 100 ppb.

2.3.1. APPI-P FTICR-MS method

The samples were analyzed using a 12 T Bruker SolariX FTICR-MS instrument. Whole oil and fractions were diluted to 0.25 mg/mL in toluene and then infused into the ionization source using a syringe pump set to deliver 200 µL/h. Atmorpheric pressure photoionization in positive ion mode via a krypton lamp at 10.6 eV was used to ionize the samples. Transfer capillary temperature and nebulizer pressure were set to 350 °C and 1.0 bar, respectively. Reserpine ($C_{33}H_{40}N_2O_9$) was added to the sample solution to assess internal calibration efficiency. The instrument was tuned using a reference Athabasca whole bitumen sample. Ions ranging from *m/z* 150 to 1500 were isolated using a linear quadrupole and accumulated over 5 ms in the collision cell before being transferred to the ICR cell. Spectra were collected in absorption mode, using an algorithm proposed elsewhere (Kilgour et al., 2013). Two hundred transients of 8 million points in the time domain were collected and summed to improve the experimental signal/noise ratio (SNR). FTICR–MS raw data were processed using the CaPA v.1.0 (Aphorist Inc.) software package. Peaks with SNR higher than 4 were assigned based on highly accurate *m/z* measurements and on stable isotopic distributions. Compositional boundaries, in terms of stoichiometry (element atom content) for the fitting algorithm, were set to $C_{4\text{-}95}H_{0\text{-}200}N_{0\text{-}2}S_{0\text{-}8}O_{0\text{-}5}$ and double bond equivalent (DBE) range, which is a measure of hydrogen deficiency due to double bonds and/or cyclic structures, was limited to be between 0 and 60. The mass spectra were recalibrated using homologous series present in the samples. Ragnarök v.2.0 (Aphorist Inc.) was used for data manipulation and visualization.

2.3.2. APPI-P FTICR-MS/MS method

A set of peaks found in the oils were selected for MS/MS experiments (Sections 4.3, 4.4 and 4.7). Sulfur-bearing parent ions were isolated (*m/z* ± 0.4) in the linear quadrupole and accumulated over 0.3–1.0 s in the collision cell. The collision cell voltage was set to 12–20 V (compared to regular operating levels at 5 V) to achieve collision-induced dissociation (CID) conditions, causing the ions to undergo several low energy collisions with room temperature argon atoms. Ions in the collision cell (parent and daughters) were then transferred to the ICR cell and the MS/MS spectra were collected in absorption mode after summing two hundred transients of 4 million points in the time domain. The instrument was tuned to detect ions ranging from *m/z* 150 to 1500, i.e. small molecular fragments (<*m/z* 150) fell outside the

analytical window in these experiments. Bruker DataAnalysis v.4.4 and R v.3.4.0 software packages were used for data processing and visualization.

3. Results

3.1. NPMF fractionation

The NPMF fractions represented 18 and 22 wt % of the Jianghan and Rozel Point oils, respectively, and their APPI-P mass spectra are shown in Figure 1.

3.2. APPI-P FTICR-MS of oils and their fractions

In all spectra acquired in this study, the isotopic pattern of ^{13}C peaks indicated the presence of singly charged species only. Averaged mass resolution (m/Δm50%) achieved for peaks detected between *m/z* 397 and 403 was higher than 1,015,000 and higher than 560,000 for peaks between *m/z* 797 and 803. Unique molecular formulas with absolute assignment error lower than 750 ppb were assigned to 40,967 monoisotopic peaks present in the oil samples spectra (Fig. 1). In each sample, peaks left unassigned represented less than 3% of total peak intensity and are not discussed further. Heteroatom classes with fewer than 25 peaks were also excluded from the discussion.

Fig. 2 shows the heteroatom class distribution of the investigated oils, as obtained by APPI-P FTICR-MS, where radical ion classes are differentiated from protonated ones by a dot following the class symbol. The relative sulfur number distribution for the studied oils, as measured in classes $S^{\bullet}_{1\text{-}6}$, is shown in Fig. 3A. Figs. 3B and 3C show the carbon number and DBE distribution of all detected molecular formulae within the oil set. Fig. 4 highlights the DBE distribution within the sulfur containing heteroatom classes, whereas Fig. 5 shows the carbon number distribution of heteroatomic classes $S^{\bullet}_{1}$ DBE 5 and 6 species. Fig. 6 shows the carbon number distribution of heteroatomic classes S_1 DBE 1 and $S^{\bullet}_{1}$ DBE 3. Fig. 7 shows the DBE distribution of C_{40} species within class $S^{\bullet}_{1\text{-}5}$ as found in Rozel Point and Jianghan oils, whereas Fig. 8 shows the heteroatomic class $S^{\bullet}_{1}$ DBE 8 carbon distribution for the same oils.

3.3. APPI-P FTICR-MS/MS

CID experiments were set to investigate the fragmentation patterns of a few selected parent ions by measuring fragments with *m/z* > 150. Fig. 9 shows a representation of the APPI-P FTICR-MS/MS spectra of class S_1 DBE 5 C_{27-30} species analyzed in the JH and RP oils, whereas Fig. 10 highlights data obtained from APPI-P FTICR-MS/MS spectra of class $S•_2$ DBE 11 $C^{\#}_{56-57}$ species.

4. Discussion

4.1. NPMF and sulfur-bridged (macro)molecules

The current understanding of organic matter sulfurization mechanisms assumes the substitution of functional groups in the precursor molecules by sulfur atoms, which then can rearrange to more stable forms such as thiolanes and thiophenes, and/or act as bridges linking two precursor molecules. As the diagenesis progresses, such linkages would propagate and eventually generate a Type II-S kerogen, which can produce oil molecules at a much lower level of thermal stress than other kerogen types (Tegelaar et al., 1989; Vandenbroucke and Largeau, 2007).

Adam et al. (1993) reported a hexane soluble nonpolar macromolecular fraction (NPMF) occurring in sulfur rich oils (including the RP oil), composed of highly aliphatic, high molecular weight structures, possibly cross-linked by sulfur in a process similar to natural vulcanization. Through a stepwise selective sulfur removal procedure, Richnow et al. (1993) proposed that in RP oil, *n*-alkanes, hopanoids, steroids and phytanes are bound simultaneously via oxygen, sulfur and aromatic units, based on the position of the functionality in the precursor molecules, creating a macromolecular matrix. Alcohols released in the desulfurization of RP oil NPMF can be as abundant as hydrocarbons; they exhibited similar carbon number distribution to hydrocarbons, but the origin of most species could not be assigned (Jenisch-Anton et al., 1999). Efforts to chemically or physically degrade such macromolecular organic matter were needed to circumvent the inefficiency of gas chromatography in analyzing sulfur rich macromolecules (Jenisch-Anton et al., 1999). Investigating the RP oil, Adam et al. (1993) reported the presence of a NPMF composed of cross-linked molecules containing multiple sulfur atoms, which represented up to 32 wt% of the whole material (Adam et al., 1992; Jenisch-Anton et al., 1999). Significantly different average molecular weight values of NPMF from RP oil were reported using various techniques (Adam et al., 1993): 815 Da by vapor pressure osmometry; 3400 Da by light scattering measurements and 1660 Da by size exclusion chromatography.

Despite a minor clean up of non-S-bearing heteroatom classes that was applied during sample preparation, FTICR-MS spectra of NPMF fractions of JH and RP oils analyzed in this study are very similar to the respective whole oil spectra (compare panels A vs. B and C vs. D in Fig. 1), indicating that the analyses of whole oils by APPI-P are representative and capture the major S-bearing constituents in those oils.

The spectra shown in Fig. 1 (A-G) revealed no detectable peaks above *m/z* 1100 in all the analyzed oils and fractions. To further corroborate the absence of high molecular weight compounds, we focused on RP oil, as illustrative of very low maturity oils, and because it has been well studied previously. An APPI-P FTICR mass spectrum was collected from *m/z* 1000–3000 (Fig. 1H), after tuning the instrument with Agilent Low Concentration Tuning mix for enhanced sensitivity at this *m/z* range. A group of peaks was detected at *m/z* 1000-1250 in Fig. 1H. Yet, no evidence could be found of larger molecules (*m/z* > 1500) in the RP oil. Considering that the NPMF is putatively formed by consecutively adding building block units, in a process similar to vulcanization, the detection of fragments at *m/z* > 1250 would be expected since a molecular size continuum should exist (Eglinton et al., 1994). The Jianghan and Rozel Point oil NPMF spectra (Fig 1B and 1D, respectively) also showed no indication of 'macromolecules' in their composition. Noteworthy, there is no evidence of in-source fragmentation, consistent with previous work by Bagag et al. (2008) on the APPI analysis of sensitive biomolecules, nor evidence of fragmentation during the ion transfer to the ICR cell. In addition, the samples fully dissolved in toluene and no evidence of molecular aggregation was seen visually or in the mass spectra. Hence, the APPI-P FTICR-MS spectra obtained herein represent a key piece in the understanding of the so called NPMF. Clearly, the APPI-P FTICR-MS results indicate that there might not be a macromolecular fraction present in RP and JH oils at all.

Intermolecular sulfur incorporation is inferred from the increased RMI detected in the C_{54-59} range within class $S•_{1}$ DBE 8 (Fig. 8), tentatively interpreted to be the indication of two C_{27-29} steroidal units bridged by one sulfur atom. Noteworthy, a similar pattern was seen in class $S•_{2-3}$ DBE 9-11 C_{54-59} species, but not in class $S•_{1}$ DBE 7. RP class $S_2•$ DBE 11 C_{56-57} compounds were selected as targets for MS/MS experiments (Fig. 10) and results show detectable daughter ions with the loss C_{28} and C_{29} with no sulfur and ΔDBE of -5.5, suggestive of an intermolecular linkage.

Although inferred, intermolecular sulfur incorporation reactions that yield high molecular weight molecules are limited. Recent investigations have recognized the impact of nanoaggregation on molecular weight measurements of other oil components, such as asphaltenes (Zhang et al., 2013). Initially thought to be as high as several thousand kilodaltons, the average molecular weights of non-aggregated asphaltene distributions are now recognized to be around 750 Da (Mullins, 2010; Hosseini-Dastgerdi et al., 2015; Snowdon et al., 2016). Similarly, the aggregation of sulfurized species might be the reason for the overestimation of NPMF molecular weights in previous studies.

4.2. Thermally immature vs. biodegraded sulfur rich oils

Sinninghe Damsté and De Leeuw (1987) used gas chromatography coupled to mass spectrometry (GC-MS), to identify not only sulfur containing isoprenoids (C_{15} and C_{20}) in Rozel Point oils but also a series of isoprenoid chains bonded to several organosulfur structures (e.g. thiophenes, thiolanes, benzothiophenes). Further work led by the same authors expanded the scope of sulfur compounds detected by GC-MS: C_{30} and C_{35} isoprenoid thiophenes, alkylthianes, isoprenoid thiolanes, thiophene steranes, thiolane steranes, alkylbenzothiophenes, isoprenoid benzothiophenes, isoprenoid bithiophenes and sulfur containing hopanoids. In total, around one thousand sulfur compounds were identified, with a molecular weight upper limit of 600 Da and a maximum of two sulfur atoms in the structure (Sinninghe Damsté et al., 1987). Such species were considered different from those sulfur compounds found in most oils since their structures are closely related to biogeochemical precursors (Sinninghe Damsté et al., 1989). Lu et al. (2014) investigated a set of Jianghan oils using ESI-P ion mode, after S-methylation reactions and detected high levels of alkyl cyclothioethers within the oils. The identified peaks ranged from classes $S_{1\text{-}3}$, DBE 1-14, and $C_{10\text{-}35}$. Compounds from class S_1 DBE 1-3 were detected with remarkably higher relative intensities. The detected predominance of $C_{20\text{-}21}$ compounds was attributed to the sulfurization of phytanic acids and phytols, and the overall sulfurization mechanism in Jianghan oils was hypothesized to involve carboxylic acids and fatty alcohols, which resulted in the formation of cyclic thioethers. Kohnen et al. (1993) identified sulfur-bound steroid and phytane moieties in the Jianghan oil (also in Rozel Point oil), suggesting that di- or polysulfide linkages are present in S-containing moieties and the position of double bonds in the precursors controls the position of S-linkages. Liu et al. (2018) showed that the ubiquitous sulfur

ring structures present in the organic sulfur compounds in Jianghan Basin oils likely originated from intramolecular sulfurization reactions.

The biogeochemistry of Peace River oils has been extensively studied in our group by Adams et al. (2013) and Bennett et al. (2013). More recently, Oldenburg et al. (2017) have shown the effects of different biodegradation levels in the chemical composition distribution in a Peace River Area, Bluesky Formation reservoir profile, as measured by FTICR-MS. Overall, molecules with higher DBE and higher sulfur number were found to be more resistant to biodegradation.

The results of this study show that the mass spectra of Jianghan and Rozel Point oils are remarkably different from the spectra of the Peace River oils (Fig. 1, A and C vs. E – G). The smoother distribution of peaks detected in the Peace River oils, similar to a bell-shaped curve, is a very common observation in fossil fuel analysis (Marshall and Rodgers, 2008) and relates to the loss of carbon number preferences caused by the thermal cracking of kerogen during oil generation. On the other hand, both Jianghan and Rozel Point oils show mass spectra that reflect a dominant signature of precursor compounds (Fig. 3C), somewhat akin to the spectra observed in recent marine sediments (Radović et al., 2016a), a consequence of the low thermal stress levels experienced by these oils. Thus, both Rozel Point and Jianghan oil APPI-P FTICR-MS mass spectra are a good representation of the chemical species and mechanisms involved in early diagenesis and related sulfur incorporation processes.

In these two oils, the predominance of heteroatom classes with one or more sulfur atoms (S_{1-6}) is evident (Fig. 2), whereas classes HC, O_{1-2}, and NO_{0-1} are the only non-sulfur containing heteroatom classes detected, accounting in total for less than 10% RMI in JH and RP oils. This is the first report of species with more than two sulfur atoms per molecule in Rozel Point oils, while Liu et al. (2018) detected up to S_5 compounds in Jianghan oils.

The Peace River oils exhibit higher RMI for S_1• species, and a decreased RMI as the sulfur number increases up to S_4• (Fig. 3A). Both Rozel Point and Jianghan oils, on the other hand, show maximum RMI at S_2• and extend up to S_6• and S_5•, respectively. Such differences may be associated with the depositional settings favoring organic matter reaction with (poly)sulfide, coupled to the low thermal stress experienced by the Jianghan and Rozel Point oils. Therefore, the relative ratios of lesser and more extensively sulfurized compound classes (e.g. S_1• vs. S_2•) is

proposed as a potentially robust proxy for source rock depositional settings, although further testing with an extended sample set is required.

Peace River oils WC and BS show very similar chemical composition (Figs. 2 and 3). Despite showing a similar carbon number distribution to its Peace River analogs in Fig. 3C, the Peace River GR oil DBE distribution is significantly shifted towards lower DBE values (Fig. 3B), while exhibiting a relative enrichment in S_2• species (Fig. 3A). Geochemical differences among the Peace River oils studied herein have been observed before by Adams et al. (2013), including a lower thermal maturity, lower biodegradation extent and higher sulfur content for oils primarily sourced from the sulfur enriched Gordondale Formation.

4.3. Sulfurized steroids and hopanoids (class S_1• DBE 5-6)

In a study by Lu et al. (2013), C_{28-30} DBE 5-7 steroids were detected in class S_1 of a sulfur rich heavy oil in Jiaxian Sag, Bohai Bay Basin, China. Sulfurized steroidal structures were previously reported in RP oil as part of the macromolecular matrix through a sulfur linkage located in ring A or B (Adam et al., 1992). Thiophene and thiolane steranes have been identified in RP oil by Sinninghe Damsté et al. (1987). Using selective cleavage of acyclic sulfide by superheated methyl iodide, Schouten et al. (1993) described the release of C_{27-30} steroid products from RP polar and asphaltene fractions. Kohnen et al. (1993) suggested that multiple substrates prone to sulfur incorporation reactions, such as Δ2-, Δ3-, Δ5-sterenes or Δ3,5-steradienes, give rise to a large variation in the positions and stereochemistry of sulfur incorporated steroids and that timing of sulfur incorporation during diagenesis would significantly influence the resulting products.

As can be observed in both in the overall (Fig. 3B) and class S_1• (Fig. 4A) DBE number distribution plots, there is a high RMI of DBE 5-6 species in Rozel Point and Jianghan oils. C_{27-30} species largely dominate the class S_1• DBE 5 carbon number distribution (Fig. 5A). Since DBE 4 species do not show an evident RMI increase for C_{27-30} in any compound classes (except for HC•), sulfurized steroid-like compounds likely include a cyclothioether moiety to result in a DBE 5 value (Fig. 5A). Although present, C_{27-30} species do not exhibit an increased RMI within heteroatom classes with more than 2 sulfur atoms. This suggests that less functionalized molecular precursors such as steroids yield less sulfur altered diagenesis products, in contrast to

386 precursors such as carotenoids that have multiple reactive sites for sulfur incorporation (Section
387 4.5).

388 The prominent class S_1• DBE 6 C_{35} peak (Fig. 5B) may represent S-bound C_{35} homohopanes,
389 which are known to be the dominant triterpene in the Rozel Point oil. The increased RMI of class
390 S_1• DBE 6 C_{27-29} species in RP oil is remarkable (Fig. 5B) because there have been no reports of
391 S-bound norhopanes despite the occurrence of S-bound (homo)hopanes in thermally immature
392 sedimentary organic matter. Within the most plausible routes for the production of sulfurized
393 steroids in natural environments (Lu et al., 2013), none would yield S-steroid species with DBE
394 6. To further investigate the forgoing interpretations, ions from class S_1• DBE 5 C_{27-30} were
395 selected as targets for MS/MS experiments (Fig. 9). In both RP and JH oils, detected daughter
396 ions represent the loss of C_{1-6} fragments with ΔDBE -0.5, i.e. aliphatic moieties such as -CH_3, -
397 C_2H_5, and no sulfur atoms, compatible with a side carbon chain fragmentation from a D-ring or
398 an AB-ring sulfurized steroid (Lu et al., 2013). The RP oil targeted ions show, although with low
399 relative intensity, ΔC_{0-2} ΔS_1 daughter ions, which indicate that some class S_1• DBE 5 C_{27-30}
400 isomers might have thiol (ΔC_0 ΔS_1 fragments) or aliphatic sulfide (ΔC_{1-2} ΔS_1) as functional
401 groups, instead of cyclic sulfide. In such cases, the parent DBE 5 ion could represent, among
402 other structures, either a 5-ring moietie (e.g. hopanoids) or a 4-ring structure with one carbon-
403 carbon double bond (e.g. sterenes). However, to the best of our knowledge, no sterenes have
404 been detected in RP oil, despite being thermally immature.

405 *4.4. Class S_1 DBE 1 and class S_1• DBE 3 species*

406 Previous work from Lu et al. (2014) indicated that the Jianghan oils are relatively enriched in
407 Class S_1 DBE 1-3 species, and the same pattern was observed herein (Figs. 4A,B). The high
408 RMI of class S_1 DBE 1 species suggests an enrichment in thiolanes or thianes, whereas high
409 RMI of class S_1• DBE 3 species suggest thiophenic structures. There is an even/odd
410 predominance spanning C_{16-40} class S_1 DBE 1 species in Jianghan oil (Fig. 6A). Lu et al. (2014)
411 reported the occurrence of odd/even predominance in the Jianghan oil class S_1, centered around
412 the C_{21} peak. Although not discussed in their paper, the methylation reactions used by Lu et al.
413 (2014) to facilitate ESI-P detection of sulfur species added one carbon to all the species detected
414 in their study, and this might have caused the reversal of actual even/odd carbon preference to
415 observed odd/even preference in their data. In agreement with our observations, Sinninghe

Damsté et al. (1987) and Sheng et al. (1987) reported a series of $C_{10\text{-}32}$ alkylthiolanes and alkylthianes in Rozel Point and Jianghan oils, respectively, which also exhibited a strong even/odd preference. Herein, the APPI-P results show that the even/odd preference extends much further, up to C_{40} in the Jianghan oil (Fig. 5A).

CID experiments were set to investigate the fragmentation patterns of class S_1 DBE 1 $C_{26,28,30}$ species. However, the experiments failed to produce any detectable daughter ion at $m/z > 150$. Typically, CID promotes the rupture of the weakest bonds in a molecule, therefore the intermediate species generated after C-S bond cleavage in thiolanes/thianes might have undergone extensive fragmentation. Based on the same reasoning, the presence of aliphatic thiols or dialkyl sulfides contributing to class S_1 DBE 1 species cannot be precluded, although the lack of class S_1 DBE 0 species indicates such functional groups may be largely absent in the oil matrices. Initially thought as intermediates in the formation of thiophenes, thiolanes have been detected in sediment extract but their association with thiophene formation is yet unclear (Sinninghe Damsté et al., 1986). The APPI-P FTICR-MS results support the hypothesis that (a) these cyclic sulfides, formed during very early stages of diagenesis, likely never partake in the kerogen formation (Brassell et al., 1988; Peng et al., 1998); and that (b) these cyclic sulfides may be derived from the same functionalized precursors as the *n*-alkanes, such as *n*-alkanoic acids and *n*-alkanols (Brassell et al., 1988; Liu et al., 2018).

Class S_1• DBE 3 species, which putatively represent thiophenic structures, show increased RMI at $C_{20,30,35,40,45}$ in the Rozel Point oil, and at $C_{20,24\text{-}26,28,30,40}$ in the Jianghan oil (Fig. 5B). FTICR-MS data alone is not capable of distinguishing isomers, but the increased RMI of multiple isoprene units (x*C_5 units) may indicate the detection of an extended range of isoprenoid thiophenes. To support this reasoning, isoprenoid thiophenes with < 35 carbons have been identified by GC-MS in Rozel Point and Jianghan oils, as reported by Sinninghe Damsté et al. (1987) and Sheng et al. (1987), respectively.

4.5. C_{40} species

The overall carbon distribution plot (Fig. 3C) shows a high RMI for C_{40} species in both RP and JH oils. This observation alone suggests the presence of compounds of biological provenance rather than produced by thermal cracking of kerogen, which typically smooths out any carbon

number preference (e.g. even/odd preference). Carotenoids are the likely biological source for C_{40} species, since they are common constituents of several living organisms, from archaea and cyanobacteria to higher plants and animals (Walter and Strack, 2011). Recently, we have used a similar APPI-P FTICR-MS approach to characterize carotenoids in recent marine sediments, in addition to various other lipid markers (Radović et al., 2016a). Whereas $C_{27\text{-}30}$ S-bearing steroids appear to be limited to classes $S_{1\text{-}2}$ (see Section 4.3.), C_{40} S-carotenoids are seen in classes with up to six sulfur atoms. Such findings indicate the clear dependence of the degree of sulfur incorporation on the number of double bonds present in the lipid undergoing diagenesis, and support the observations and interpretations reported previously with ESI FTICR-MS data (Liu et al., 2018). Carotenoids can offer multiple spots for sulfur incorporation, contrary to steroids which have a limited number of double bonds and oxygenated groups. The predominance of C_{40} in classes $S_{5\text{-}6}$• is remarkable and reveals that, overall, most of the sulfurized species may resemble the biological precursors in both Jianghan and Rozel Point oils.

Typical carotenoid structures (e.g., lycopene, β-carotene, nostoxanthin) have 13 DBE units, although higher DBE species are also possible (Walter and Strack, 2011). Carotenoid diagenesis in different depositional settings can be quite complex (Watts and Maxwell, 1977; Repeta and Gagosian, 1987), but the identification of several reduced carotenoids in recent sediments suggests that hydrogenation occurs during diagenesis without structural or stereochemical specificity (Hebting et al., 2006). Adam et al. (1993) not only suggested acyclic carotenes, β-carotene and monocyclic carotenes as building blocks of Rozel Point NPMF, but also discussed their implications to organic matter input determination. In the current study, similarly to Liu et al. (2018), sulfurized carotenoids are present in the oils as free molecules instead of being building blocks of NPMF, as evident by the absence of cross-linked carotenoid-derived NPMF intermediates (i.e., no significant signal from C_{80} species was detected). In summary, the sulfur incorporation in carotenoid precursors is not followed by an increase in the carbon number, thus mostly original (biological) C_{40} species with varying DBE values were detected.

Fig. 8 shows the DBE distribution of classes $S_{1\text{-}5}$• C_{40} species. A significant pattern observed in Fig. 8 is the increased RMI for the DBE = S + (2,4,6) species, which might reflect the level of 'thiophenization'. That is, DBE = S + 0 species would represent altered aliphatic carotenoids (e.g. lycopene) where the sulfur atoms are incorporated as thiolane. DBE = S + 2 species

represent the altered carotenoids with 2 cyclic structures (e.g. beta-carotane) where sulfur atoms are incorporated as thiolane. Note the higher RMI of DBE S + 2 compared to DBE S + 0 species, reflecting the higher abundance of cyclic carotenoid structure in the deposited organic matter. Since the conversion of a thiolane into thiophenes involves a ΔDBE +2 shift, species with DBE S + 4 and S + 6 may reflect the number of thiophenic structures present in the compound. The transformation of thiolanes into thiophenes is likely dependent on the thermal stress level experienced by the sample. The ratios of thiophene and thiolane structures within the carotenoid classes require further investigation to determine its potential usefulness as a marker for early diagenesis sulfurization.

4.6. The DBE number ≥ S_x rule

In Fig. 8, the minimum detected DBE number in each plot is equal to the number of sulfur atoms of the corresponding class, i.e. DBE number ≥ S_x, which indicates that, for C_{40} assignments, the sulfur incorporation reactions are associated with a DBE increase. In fact, such a pattern is observed in the dominant molecular formulae detected in this study, indicating that polysulfides, aliphatic sulfides and thiols must be largely absent as stand-alone functional groups in the RP and JH oils. The only exceptions to the rule are class S_2• DBE 1 $C_{16,18,20,22,24,26}$ and class S_3• DBE 2 C_{37} species. The even/odd predominance in class S_1 DBE 1 was discussed previously. The species in class S_2• DBE 1 $C_{16,18,20,22,24,26}$ probably relates to those where an additional sulfur atom is incorporated as a cyclic polysulfide or a thiol. The class S_3• DBE 2 C_{37} species are discussed in Section 4.7.

4.7. Sulfurized alkenones

Alkenones are long chain unsaturated ketones produced by some phytoplankton species and typically used as paleoenvironmental proxies (Volkman et al., 1980; Brassell et al., 1986). An increased RMI was observed for classes $S_{1\text{-}3}$• DBE 1-3 C_{37} species in Rozel Point oil, suggesting that alkenones have also undergone sulfurization during diagenesis. Although it is tempting to try and estimate the ratios of parent $C_{37:2}$ and $C_{37:3}$ (e.g. UK`37) based on their sulfurized analogs, this exercise would be highly speculative at this point. Also, the occurrence of class S_3• DBE 2 C_{37} species as an exception to the DBE number ≥ S_x rule, indicates that in some cases thiol or polysulfides might be present. The peak representing class S_2• DBE 2 C_{37} in Rozel Point oil was

selected for MS/MS experiments, and similarly to class S_1 DBE 1 peaks, no daughter ions could be detected, except for an ion representing the loss of a -SH group. This result suggests that the C_{37} assignments investigated herein may display long alkyl chains, which in turn produce daughter ions which undergo further fragmentation, leaving our analytical window at *m/z* >150.

4.8. Implications for atmospheric carbon dioxide removal

To meet the challenges of climate predictions at the end of the 21st century (IPCC, 2018), technologies will be needed that remove carbon dioxide from the atmosphere and sequester it for geological time frames. Such processes, termed carbon dioxide removal (CDR) are increasingly attracting both research and commercial investment interest. Only a few CDR technologies are currently being commercially developed, e.g. bio-energy with carbon capture and storage, or direct air capture, but are still far below the scale needed for globally significant CO_2 reduction, which would require achieving carbon drawdowns in the order of 100 to 1000 Gt by the year 2100 (IPCC, 2018). A better understanding of natural mechanisms for long term preservation of organic molecules can provide guidelines for the development of technologies that could leverage those mechanisms to artificially enhance the removal of carbon in the geosphere in the form of engineered organic species. We term these species “alternative vectors for carbon storage”, or AVECS for short, and are currently investigating several routes to produce AVECS from organic precursors, including pathways involving sulfurization of organic molecules (Yim, 2019). To that end, the study reported herein provided multiple indications relevant to AVECS technology development issues such as:

- Natural precursors such as pigments or lipids can incorporate sulfur as free molecules;
- Double bonds are the key molecular site for sulfur incorporation;
- Given the fact that double bonds are quite reactive, the sulfur incorporation must be taking place early in the diagenesis, at low pressures and temperatures, which favorably implies fewer energy needs for AVECS production;
- Cyclization is the favored sulfur incorporation mechanism producing thiolane structures, which can then be aromatized to thiophenes during diagenesis.

Some of these processes can be modelled and reproduced in the laboratory (Yim, 2019), however much more research effort will be needed to move these types of reactions from bench-scale to

sustainable pilot or large-scale deployments; notwithstanding, biogeochemical processes occurring in geosphere, such as those inferred from the current study of sulfur rich oils, can provide valuable insights and lessons which can direct this type of research.

5. Conclusions

The present study leveraged the expanded analytical window offered by novel analytical technologies to improve the current geochemical understanding of diagenetic processes involving sulfur and the resultant occurrence of sulfur rich oils. A set of five sulfur rich oils was analyzed via APPI-P FTICR-MS(/MS) and the following conclusions were drawn from the results:

The absence of peaks at $m/z > 1250$ in Rozel Point and Jianghan oils, as well as in their non-polar macromolecular fractions, disproves the previously established concept of a macromolecular network linked by (poly)sulfide bridges, which has been proposed to explain the occurrence of non-GC-MS amenable sulfur compounds in immature, sulfur rich oils. Instead, it appears that the presence of highly sulfurized lipids (up to six sulfur atoms) as free molecules are the result of sulfurization that in turn depends on the abundance of functional groups (double bonds mainly) in the precursor molecules.

Source rock thermal stress levels were found to be a key factor differentiating the composition of biodegraded, sulfur rich Peace River oils, compared to thermally immature, sulfur rich Rozel Point and Jianghan oils. Whereas Peace River oils do not show biological precursor skeleton signatures, Rozel Point and Jianghan oils show the presence of S-containing steroids, hopanoids, carotenoids and alkenones among others.

APPI-P FTICR-MS/MS experiments indicated only a minor occurrence of thiol functional groups and sulfide bridges linking two precursor molecules. The compositional patterns observed in sulfurized C_{40} assignments, representing S-bound carotenoids, supports a mechanism of sulfur incorporation involving the formation of thiolane structures, which can then be aromatized to thiophenes during diagenesis. FTICR-MS/MS experiments were also helpful to prove the occurrence of intermolecular sulfur incorporation reactions as a secondary mechanism, the aliphatic nature of class S_1 DBE 1 species and sulfurized alkenones, the preference of cycle-

forming sulfur incorporation in steroid structures, and the occurrence of thiol/thioether groups, although these were seen only to a minor extent.

The analytical approach presented herein can be improved and expanded by using analytical workflows that include chromatographic separation to better characterize individual molecular species, as well as by including other sample types such as source rocks and recent sediments to better constrain the progression of diagenetic processes involving sulfur incorporation.

The occurrence of S-bound compounds in oils or sediment extracts, as detected via FTICR-MS, can be used as proxies for depositional environment, organic matter input, sulfurization and other diagenetic processes. Understanding the relationship between the precursor and sulfurized products, as well as the mechanisms for such reactions, is key to the design of geoengineering solutions to enhance carbon preservation in the geosphere by promoting sulfurization of biomass.

AUTHOR INFORMATION

Corresponding author

*Telephone: +1 403 210.3916. Fax: +1 403 220.8618. E-mail: rcsilva@ucalgary.ca

Notes

The authors declare no competing financial interest.

ACKNOWLEDGEMENTS

This research was made possible in part by research support from Canada First Research Excellence Fund (CFREF), UCalgary Global Research Initiative in Low Carbon Unconventional Resources, Foundation for Innovation (CFI), the Natural Sciences and Engineering Research Council of Canada (NSERC), PRG and the University of Calgary. Aphorist Inc. and Ryan W. Snowdon are acknowledged for software support.

This study was conceived of and designed by RCS, CY and SRL with key input from JR and TBPO. CY carried out literature reviews, laboratory experiments, data interpretation and contributed to writing. FTICR-MS method optimization and analyses were carried out by MB,

and data processing and interpretation were carried out by RCS. PW assisted with the NPMF fractionation. JRR contributed to data interpretation and manuscript writing. HH, LRS and TBPO assisted with sample collection and geochemical discussions on the petroleum systems aspects and prior FTMS studies of high sulfur oils. All authors revised the manuscript.

References

Adam, P., Mycke, B., Schmid, J.C., Connan, J., Albrecht, P., 1992. Steroid moieties attached to macromolecular petroleum fraction via di- or polysulphide bridges. Energy & Fuels 6, 553-559.

Adam, P., Schmid, J.C., Mycke, B., Strazielle, C., Connan, J., Huc, A., Riva, A., Albrecht, P., 1993. Structural investigation of nonpolar sulfur cross-linked macromolecules in petroleum. Geochimica et Cosmochimica Acta 57, 3395-3419.

Adams, J., Larter, S., Bennett, B., Huang, H., 2012. Oil charge migration in the Peace River oil sands and surrounding region. Abstract. GeoConvention 2012: Vision, Calgary.

Adams, J., Larter, S., Bennett, B., Huang, H., Westrich, J., & Kruisdijk, C. v. 2013. The Dynamic Interplay of Oil Mixing, Charge Timing, and Biodegradation in Forming the Alberta Oil Sands: Insights from Geologic Modeling and Biogeochemistry, In: Hein, F. J., Leckie, D., Larter, S., Suter, J. R. (Eds.), Heavy-Oil and Oil-Sand Petroleum Systems in Alberta and Beyond. American Association of Petroleum Geologists.

Aizenshtat, Z., Krein, E.B., Vairavamurthy, M.A., Goldstein, T.P., 1995. Role of Sulfur in the Transformations of Sedimentary Organic Matter: A Mechanistic Overview, in: Geochemical Transformations of Sedimentary Sulfur, ACS Symposium Series. American Chemical Society, pp. 2–16.

Allan, J., Creaney, S., 1991. Oil families of the Western Canada basin. Bulletin of Canadian Petroleum Geology 39, 107-122.

Amrani, A., 2014. Organosulfur compounds: Molecular and isotopic evolution from biota to oil and gas. Annual Review of Earth and Planetary Sciences 42, 733-768.

Bagag, A., Giuliani, A., Laprévote, O., 2008. Atmospheric pressure photoionization mass spectrometry of oligodeoxyribonucleotides. European Journal of Mass Spectrometry 14, 71.

Bennett, B., Adams, J.J., Gray, N.D., Sherry, A., Oldenburg, T.B.P., Huang, H., Larter, S.R., Head, I.M., 2013. The controls on the composition of biodegraded oils in the deep subsurface – Part 3. The impact of microorganism distribution on petroleum geochemical gradients in biodegraded petroleum reservoirs. Organic Geochemistry 56, 94-105.

Brassell, S.C., Eglinton, G., Marlowe, I.T., Pflaumann, U., Sarnthein, M., 1986. Molecular stratigraphy: A new tool for climatic assessment. Nature 320, 129-133.

Brassell, S.C., Eglinton, G., Sheng, G., Fu, J., 1988. Biological markers in lacustrine Chinese oil shales. Lacustrine Petroleum Source Rocks 40, 299-308.

Carroll, A., Bohacs, K., 2001. Lake-type controls on petroleum source rock potential in nonmarine basin. American Association of Petroleum Geologists Bulletin 85, 1033-1053.

Eglinton, T.I., Irvine, J.E., Vairavamurthy, A., Zhou, W., Manowitz, B., 1994. Formation and diagenesis of macromolecular organic sulfur in Peru margin sediments. Organic Geochemistry 22, 781-799.

Hansell, D.A., Carlson, C.A., Repeta, D., Schlitzer, R., 2009. Dissolved organic matter in the ocean: New insights stimulated by a controversy. Oceanography 22, 202-211.

Hebting, Y., Schaeffer, P., Behrens, A., Adam, P., Schmitt, G., Schneckenburger, P., Bernasconi, S.M., Albrecht, P., 2006. Biomarker evidence for a major preservation pathway of sedimentary organic carbon. Science 312, 1627-1631.

Hosseini-Dastgerdi, Z., Tabatabaei-Nejad, S.A.R., Khodapanah, E., Sahraei, E., 2015. A comprehensive study on mechanism of formation and techniques to diagnose asphaltene

structure; molecular and aggregates: A review. Asia-Pacific Journal of Chemical Engineering 10, 1-14.
Hou, Y., Wang, F., He, S., Dong, T., Wu, S., 2017. The properties and shale oil potential of saline lacustrine shales in the Qianjiang Depression, Jianghan Basin, China. Marine and Petroleum Geology 86.
Houghton, R.A., 2007. Balancing the global carbon budget. Annual Review of Earth and Planetary Sciences 35, 313-347.
Huang, C., Hinnov, L., 2014. Evolution of an Eocene-Oligocene saline lake depositional system and its controlling factors, Jianghan Basin, China. Journal of Earth Science 25, 959-976.
Hughey, C.A., Rodgers, R.P., Marshall, A.G., Walters, C.C., Qian, K., Mankiewicz, P., 2004. Acidic and neutral polar NSO compounds in Smackover oils of different thermal maturity revealed by electrospray high field Fourier transform ion cyclotron resonance mass spectrometry. Organic Geochemistry 35, 863-880.
IPCC, 2018. Global Warming of 1.5° C: An IPCC Special Report on the Impacts of Global Warming of 1.5° C Above Pre-industrial Levels and Related Global Greenhouse Gas Emission Pathways, in the Context of Strengthening the Global Response to the Threat of Climate Change, Sustainable Development, and Efforts to Eradicate Poverty. Intergovernmental Panel on Climate Change.
Jenisch-Anton, A., Adam, P., Schaeffer, P., Albrecht, P., 1999. Oxygen-containing subunits in sulfur-rich nonpolar macromolecules. Geochimica et Cosmochimica Acta 63, 1059-1074.
Jiao, N., Herndl, G.J., Hansell, D.A., Benner, R., Kattner, G., Wilhelm, S.W., Kirchman, D.L., Weinbauer, M.G., Luo, T., Chen, F., Azam, F., 2010. Microbial production of recalcitrant dissolved organic matter: Long-term carbon storage in the global ocean. Nature Reviews Microbiology 8, 593.
Kilgour, D.P.A., Neal, M.J., Soulby, A.J., O'Connor, P.B., 2013. Improved optimization of the Fourier transform ion cyclotron resonance mass spectrometry phase correction function using a genetic algorithm. Rapid Communications in Mass Spectrometry 27, 1977–1982.
Kohnen, M.E.L., Sinninghe Damsté, J.S., Baas, M., Dalen, A.C.K., de Leeuw, J.W., 1993. Sulphur-bound steroid and phytane carbon skeletons in geomacromolecules: Implications for the mechanism of incorporation of sulphur into organic matter. Geochimica et Cosmochimica Acta 57, 2515–2528.
Liu, W., Liao, Y., Shi, Q., Hsu, C.S., Jiang, B., Peng, P.a., 2018. Origin of polar organic sulfur compounds in immature crude oils revealed by ESI FT-ICR MS. Organic Geochemistry 121, 36-47.
Lu, H., Peng, P., Hsu, C.S., 2013. Geochemical explication of sulfur organics characterized by Fourier transform ion cyclotron resonance mass spectrometry on sulfur-rich heavy oils in Jinxian Sag, Bohai Bay Basin, northern China. Energy & Fuels 27, 5861-5866.
Lu, H., Shi, Q., Ma, Q., Shi, Y., Liu, J., Sheng, G., Peng, P., 2014. Molecular characterization of sulfur compounds in some specieal sulfur-rich Chinese crude oils by FT-ICR MS. Science China Earth Sciences 57, 1158-1167.
Marshall, A.G., Rodgers, R.P., 2008. Petroleomics: Chemistry of the underworld. Proceedings of the National Academy of Sciences 105, 18090-18095.
Meissner, F.F., Woodward, J., Clayton, J.L., 1984. Stratigraphic relationships and distribution of source rocks in the Greater Rocky Mountain Region. In: Woodward, J., Meissner, F.F., Clayton, J.L., (Eds.), Hydrocarbon Source Rocks of the Greater Rocky Mountain Region. Rocky Mountains Assoc. Geol. pp. 1-34.

Mullins, O.C., 2010. The modified Yen model. Energy & Fuels 24, 2179-2207.
Oldenburg, T.B.P., Brown, M., Bennett, B., Larter, S.R., 2014. The impact of thermal maturity level on the composition of crude oils, assessed using ultra-high resolution mass spectrometry. Organic Geochemistry 75, 151-168.
Oldenburg, T.B.P., Jones, M., Huang, H., Bennett, B., Shafiee, N.S., Head, I., Larter, S.R., 2017. The controls on the composition of biodegraded oils in the deep subsurface – Part 4. Destruction and production of high molecular weight non-hydrocarbon species and destruction of aromatic hydrocarbons during progressive in-reservoir biodegradation. Organic Geochemistry 114, 57-80.
Orr, W.L., Sinninghe Damsté, J.S., 1990. Geochemistry of sulfur in petroleum systems. Geochemistry of Sulfur in Fossil Fuels. American Chemical Society, pp. 2-29.
Peirong, W., Dajiang, Z., Guanjun, X., Tingrong, X., Fuqing, S., Bing, C., 2008. Geochemical features of light hydrocarbons of typical salt lake oils sourced from Jianghan Basin, China. Organic Geochemistry 39, 1631-1636.
Peng, P., Sheng, G., Fu, J., Wu, Z., Jiang, J., 1998. Origin of immature sulfur-rich oil in Jianghan oil field. Chinese Science Bulletin 43, 678-681.
Philp, R.P., Zhaoan, F., 1987. Geochemical investigation of oils and source rocks from Qianjiang depression of Jianghan Basin, a terrigenous saline basin, China. Organic Geochemistry 11, 549-562.
Pohlabeln, A.M., Gomez-Saez, G.V., Noriega-Ortega, B.E., Dittmar, T., 2017. Experimental Evidence for Abiotic Sulfurization of Marine Dissolved Organic Matter. Frontiers in Marine Science, 4.
Purcell, J.M., Hendrickson, C.L., Rodgers, R.P., Marshall, A.G., 2006. Atmospheric pressure photoionization Fourier transform ion cyclotron resonance mass spectrometry for complex mixture analysis. Analytical Chemistry 78, 5906-5912.
Radović, J., Silva, R., Snowdon, R., Brown, M., Larter, S.R., Oldenburg, T., 2016a. A rapid method to assess a broad inventory of organic species in marine sediments using ultra-high resolution mass spectrometry. Rapid Communications in Mass Spectrometry 30, 1273-1282.
Radović, J.R., Silva, R.C., Snowdon, R., Larter, S.R., Oldenburg, T.B.P., 2016b. Rapid screening of glycerol ether lipid biomarkers in recent marine sediment using atmospheric pressure photoionization in positive mode Fourier transform ion cyclotron resonance mass spectrometry. Analytical Chemistry 88, 1128-1137.
Raffaelli, A., Saba, A., 2003. Atmospheric pressure photoionization mass spectrometry. Mass Spectrometry Reviews 22, 318-331.
Raven, M.R., Sessions, A.L., Adkins, J.F., Thunell, R.C., 2016. Rapid organic matter sulfurization in sinking particles from the Cariaco Basin water column. Geochimica et Cosmochimica Acta 190, 175-190.
Repeta, D.J., Gagosian, R.B., 1987. Carotenoid diagenesis in recent marine sediments—I. The Peru continental shelf (15°S, 75°W). Geochimica et Cosmochimica Acta 51, 1001-1009.
Richnow, H.H., Jenisch, A., Michaelis, W., 1993. The chemical structure of macromolecular fractions of a sulfur-rich oil. Geochimica et Cosmochimica Acta 57, 2767-2780.
Riediger, C., 1994. Migration of "Nordegg" Oil in the Western Canada Basin. How much and how far? Bulletin of Canadian Petroleum Geology 42, 63-73.

Schouten, S., Pavlović, D., Sinninghe Damsté, J.S., de Leeuw, J.W., 1993. Selective cleavage of acyclic sulphide moieties of sulphur-rich geomacromolecules by superheated methyl iodide. Organic Geochemistry 20, 911-916.

Sheng, G., Fu, J., Brassell, S.C., Gowar, A.P., Eglinton, G., Sinninghe Damsté, J.S., de Leeuw, J.W., Schenck, P.A., 1987. Sulphur-containing compounds in sulphur-rich crude oils from hypersaline lake sediments and their geochemical implications. Chinese Journal of Geochemistry 6, 115-126.

Sinninghe Damsté, J.S., De Leeuw, J.W., 1987. The origin and fate of isoprenoid C 20 and C 15 sulphur compounds in sediments and oils. International Journal of Environmental Analytical Chemistry 28, 1-19.

Sinninghe Damsté, J.S., De Leeuw, J.W., Kock-Van Dalen, A.C., De Zeeuw, M.A., Lange, F.D., Irene, W., Rijpstra, C., Schenck, P.A., 1987. The occurrence and identification of series of organic sulphur compounds in oils and sediment extracts. I. A study of Rozel Point Oil (U.S.A.). Geochimica et Cosmochimica Acta 51, 2369-2391.

Sinninghe Damsté, J.S., Rijpstra, W.I.C., De Leeuw, J.W., Schenck, P.A., 1989. The occurrence and identification of series of organic sulphur compounds in oils and sediment extracts: II. Their presence in samples from hypersaline and non-hypersaline palaeoenvironments and possible application as source, palaeoenvironmental and maturity indicators. Geochimica et Cosmochimica Acta 53, 1323-1341.

Sinninghe Damsté, J.S., ten Haven, H.L., De Leeuw, J.W., Schenck, P.a., 1986. Organic geochemical studies of a Messinian evaporitic basin, northern Apennines (Italy)—II Isoprenoid and *n*-alkyl thiophenes and thiolanes. Organic Geochemistry 10, 791-805.

Snowdon, L.R., Volkman, J.K., Zhang, Z., Tao, G., Liu, P., 2016. The organic geochemistry of asphaltenes and occluded biomarkers. Organic Geochemistry 91, 3-15.

Summons, R., Amend, J., Bish, D., Buick, R., Cody, G., Des Marais, D., Dromart, G., Eigenbrode, J., Knoll, A., Sumner, D., 2011. Preservation of Martian organic and environmental records: Final report of the Mars biosignature working group. Astrobiology 11, 157-181.

Tegelaar, E.W., de Leeuw, J.W., Derenne, S., Largeau, C., 1989. A reappraisal of kerogen formation. Geochimica et Cosmochimica Acta 53, 3103-3106.

ten Haven, H.L., de Leeuw, J.W., Sinninghe Damsté, J.S., Schenck, P.A., Palmer, S.E., Zumberge, J.E., 1988. Application of biological markers in the recognition of palaeohypersaline environments. Geological Society, London, Special Publications, pp. 123-130.

Vandenbroucke, M., Largeau, C., 2007. Kerogen origin, evolution and structure. Organic Geochemistry 38, 719-833.

Volkman, J.K., Eglinton, G., Corner, E.D.S., Sargent, J.R., 1980. Novel unsaturated straight-chain C37-C39 methyl and ethyl ketones in marine sediments and a coccolithophore Emiliania huxleyi. Physics and Chemistry of the Earth 12, 219-227.

Walter, M.H., Strack, D., 2011. Carotenoids and their cleavage products: Biosynthesis and functions. Natural Product Reports 28, 663.

Walters, C.C., Qian, K., Wu, C., Mennito, A.S., Wei, Z., 2011. Proto-solid bitumen in petroleum altered by thermochemical sulfate reduction. Organic Geochemistry 42, 999-1006.

Walters, C.C., Wang, F.C., Qian, K., Wu, C., Mennito, A.S., Wei, Z., 2015. Petroleum alteration by thermochemical sulfate reduction – A comprehensive molecular study of aromatic hydrocarbons and polar compounds. Geochimica et Cosmochimica Acta 153, 37-71.

Watts, C.D., Maxwell, J.R., 1977. Carotenoid diagenesis in a marine sediment. Geochimica et Cosmochimica Acta 41, 493-497.

Werne, J.P., Hollander, D.J., Lyons, T.W., Sinninghe Damsté, J.S., Amend, J.P., Edwards, K.J., 2004. Organic sulfur biogeochemistry: Recent advances and future research directions. Sulfur Biogeochemistry - Past and Present. Geological Society of America.

Yim, C. 2019. Organic Sulfur-Bearing Species as Subsurface Carbon Storage Vectors (Unpublished master's thesis). University of Calgary, Calgary, AB.

Zhang, L., Shi, Q., Zhao, C., Zhang, N., Chung, K.H., Xu, C., Zhao, S., 2013. Molecular weight and aggregation of heavy petroleum fractions measured by vapor pressure osmometry and a hindered stepwise aggregation model. Energy & Fuels 27, 1331-1336.

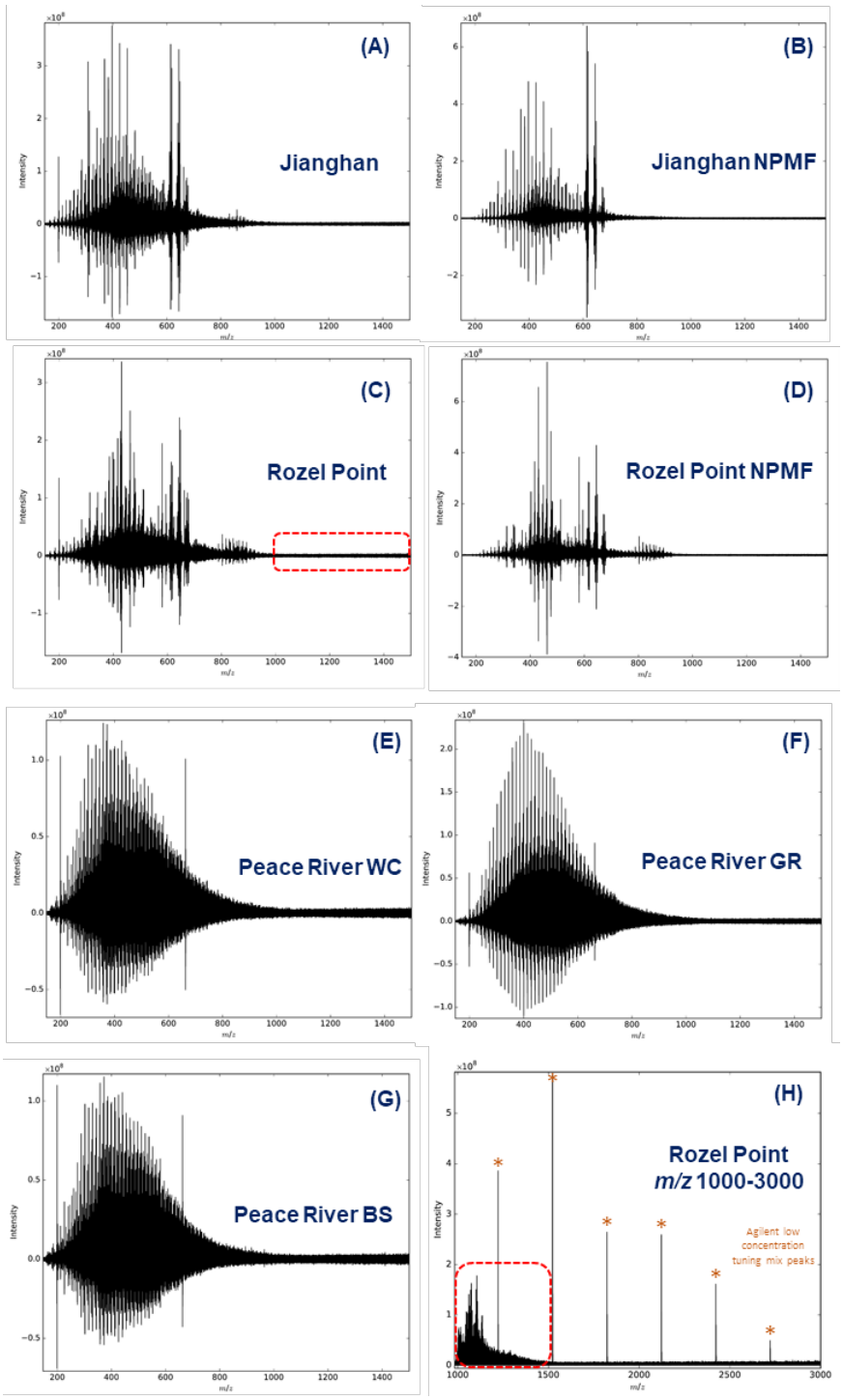

Figure 1. APPI-P FTICR absorption-mode mass spectrum of (A-B) Jianghan oil and NPMF, (C-D) Rozel Point oil and NPMF, (E-G) Peace River oils (see Table 1 for sample codes). Plot H shows the Rozel Point oil APPI-P FTICR magnitude-mode mass spectrum, acquired from *m/z* 1000 – 3000, 100 scans, ion accumulation time increased by a 100-fold (500 ms), where the sample solution was doped with 2.5 µL of the Agilent Low Concentration Tuning Mix.

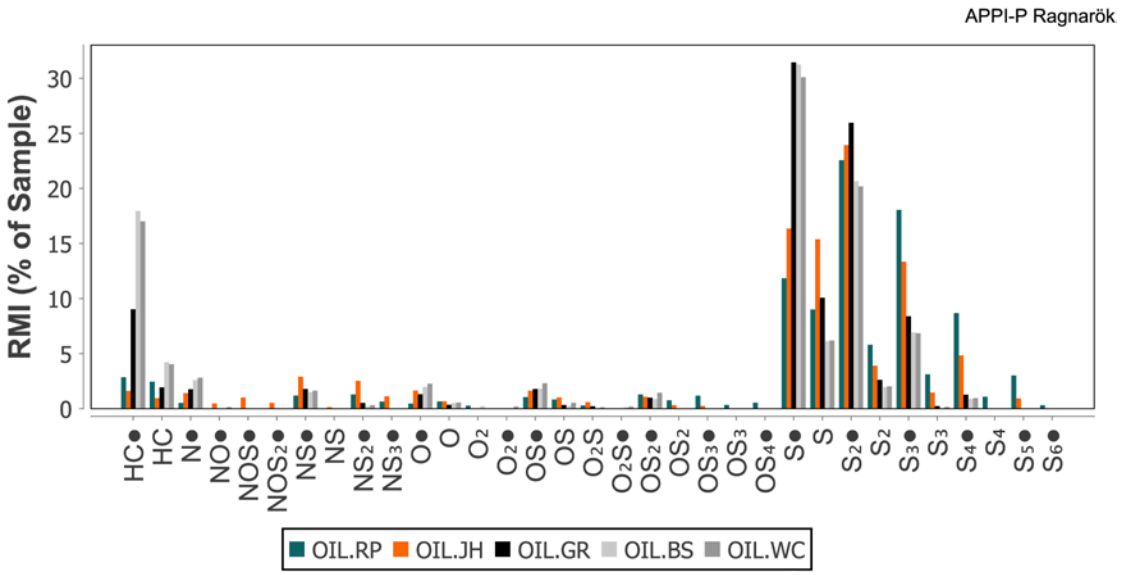

Figure 2. APPI-P FTICR-MS compound class distribution of the oil samples analyzed in this study. Dots following class labels refer to radical ions (odd electron ion) while the absence of a dot refers to protonated ions (even electron ion). The relative monoisotopic intensity (RMI, % of Sample) is calculated as the fraction of the total monoisotopic intensities of a compound class, normalized to the sum of monoisotopic intensities of all compound classes in the sample. See Table 1 for sample abbreviations.

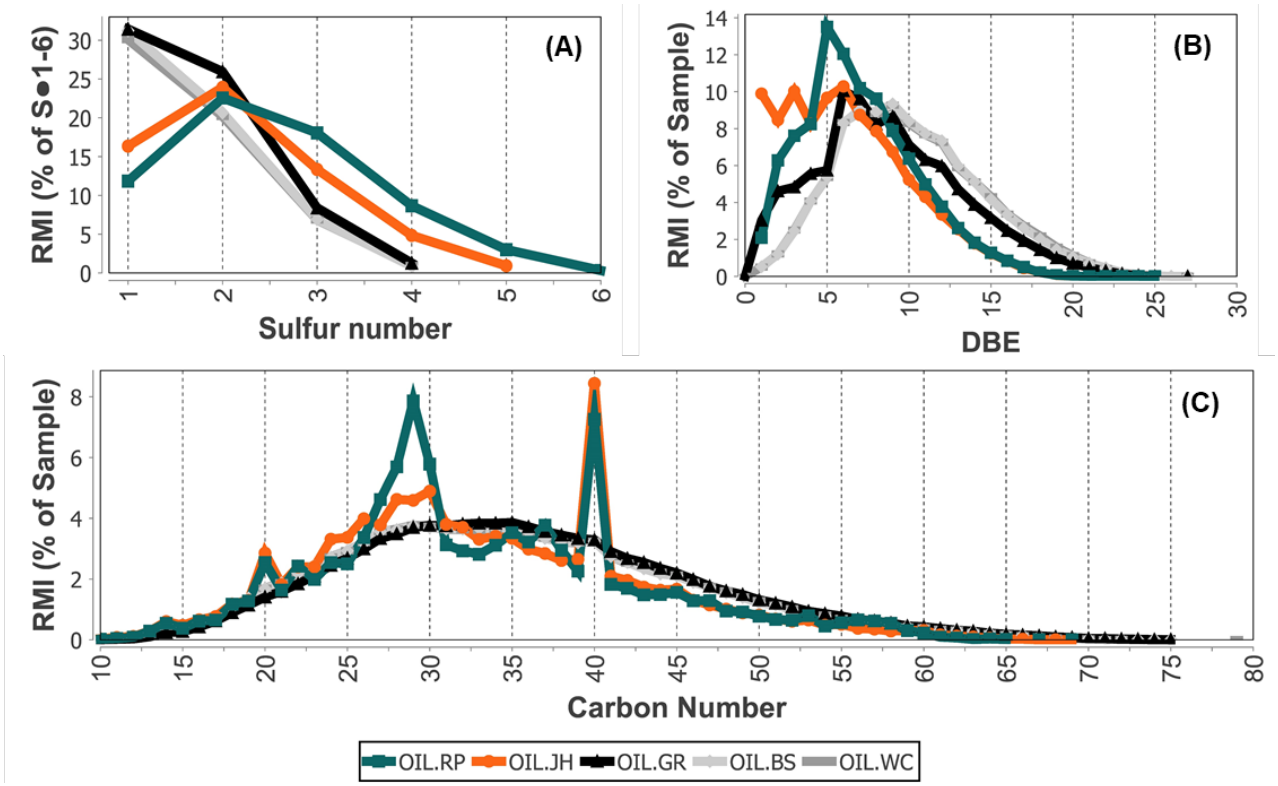

Figure 3. APPI-P FTICR-MS parameter distributions in the oil samples analyzed in this study. (A) DBE number distribution of all assigned peaks; (B) Sulfur number distribution, based on radical heteroatomic classes $S•_{1\text{-}6}$ peaks; (C) Carbon number distribution of all assigned peaks. See Table 1 for sample abbreviations.

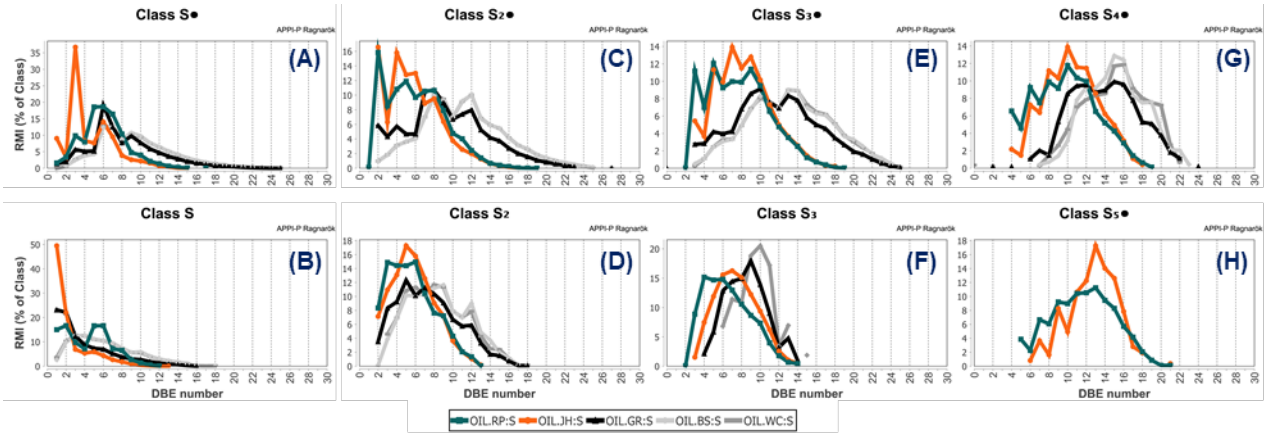

Figure 4. APPI-P FTICR-MS heteroatomic classes $S\bullet_{1\text{-}5}$ and $S_{1\text{-}3}$ DBE number distributions in the oil sample set. Dots following class labels refer to radical ions (odd electron ion) while the absence of a dot refers to protonated ions (even electron ion). See Table 1 for sample abbreviations.

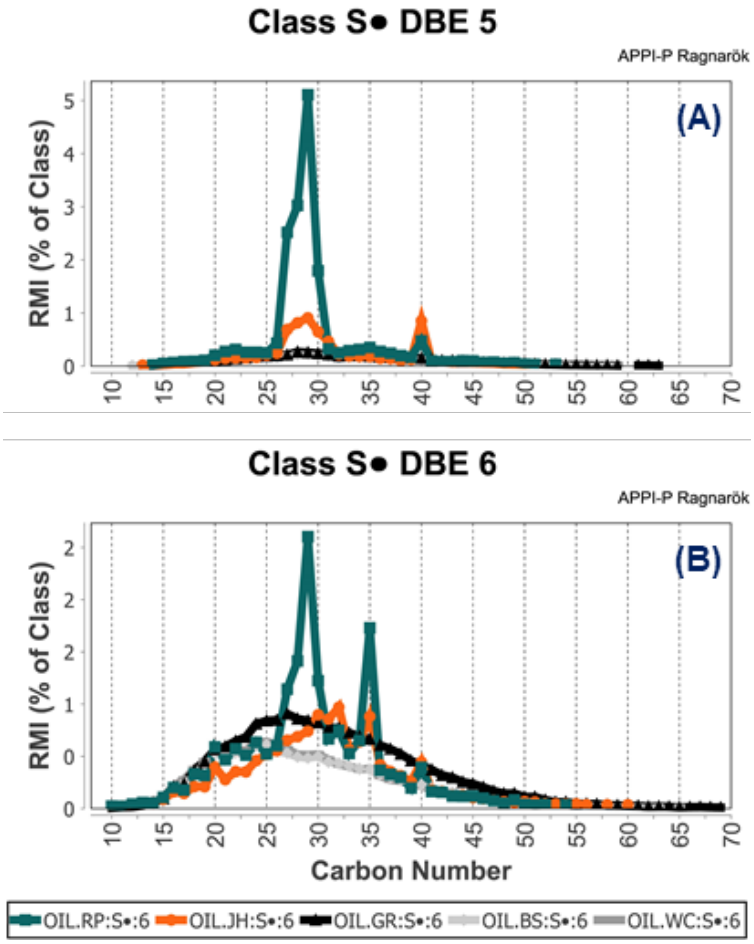

Figure 5. APPI-P FTICR-MS carbon number distribution of heteroatomic classes $S•_1$ DBE 5 (A) and 6 (B). Dots following class labels refer to radical ions (odd electron ion. See Table 1 for sample abbreviations.

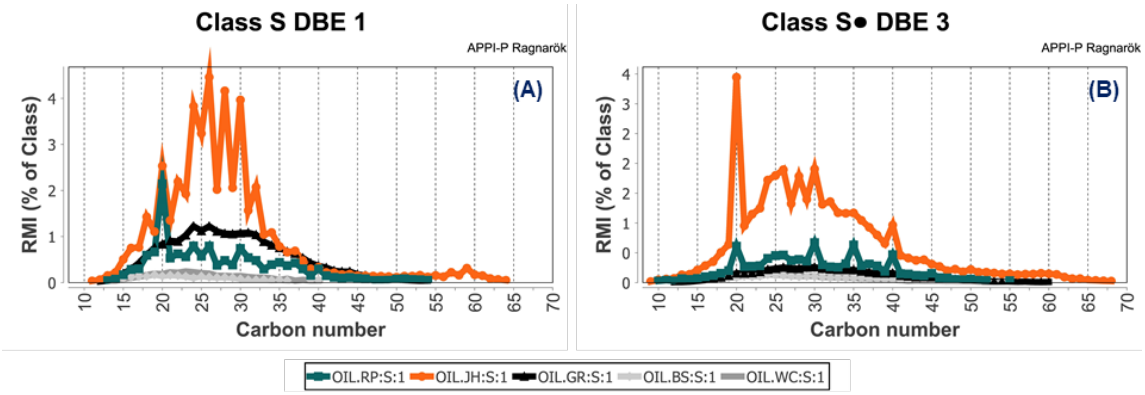

Figure 6. APPI-P FTICR-MS carbon number distribution of heteroatomic classes (A) S_1 DBE 1 and (B) $S•_1$ DBE 3. Dots following class labels refer to radical ions (odd electron ion) while the absence of a dot refers to protonated ions (even electron ion). See Table 1 for sample abbreviations.

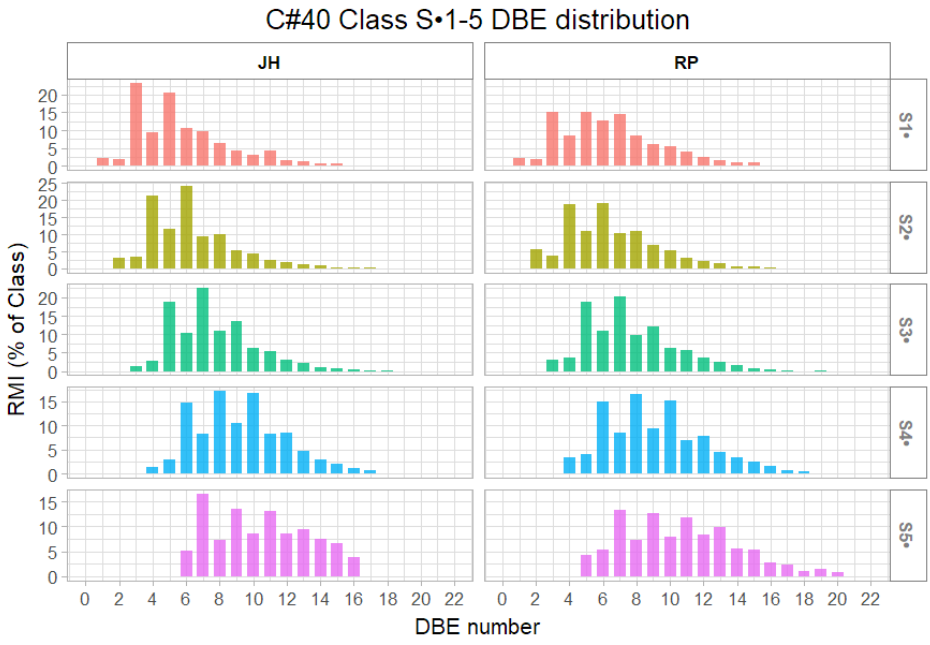

Figure 7. DBE distribution of class $S_{1\text{-}5}$• C_{40} species in Rozel Point and Jianghan oils, as detected by APPI-P FTICR-MS.

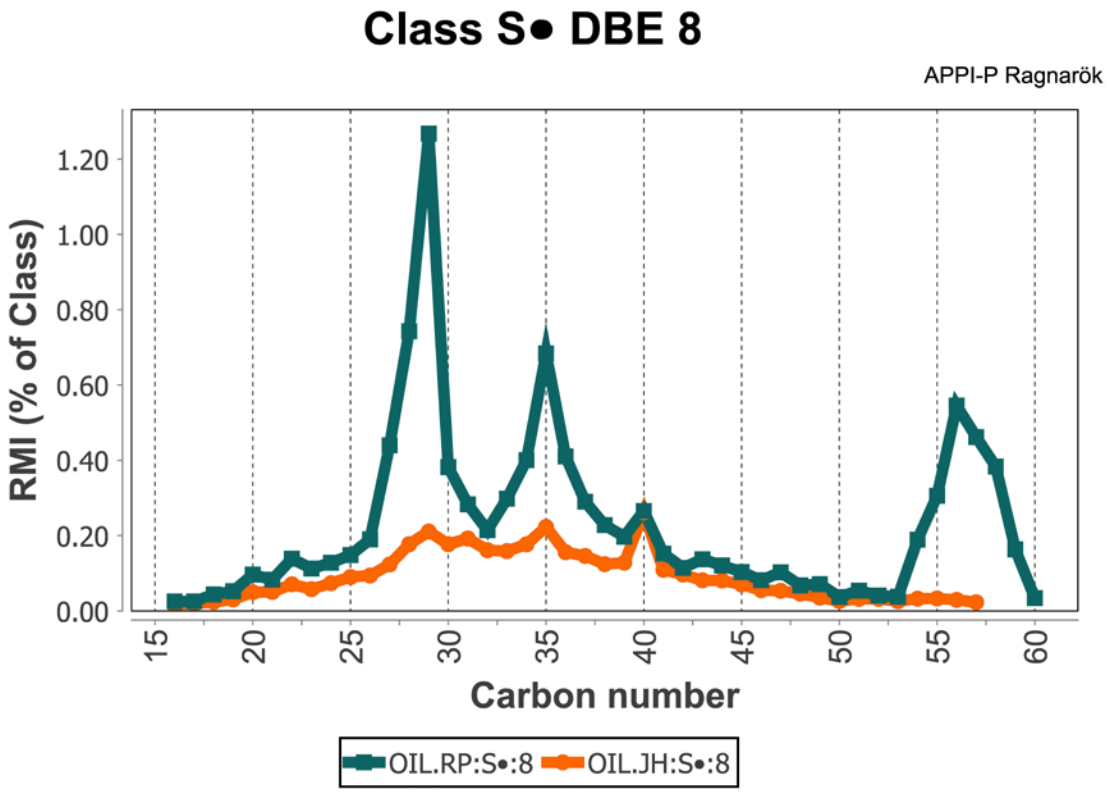

Figure 8. APPI-P FTICR-MS carbon number distribution of heteroatomic class $S•_1$ DBE 8, in Jianghan (JH) and Rozel Point (RP) oils. Dots following class labels refer to radical ions (odd electron ion).

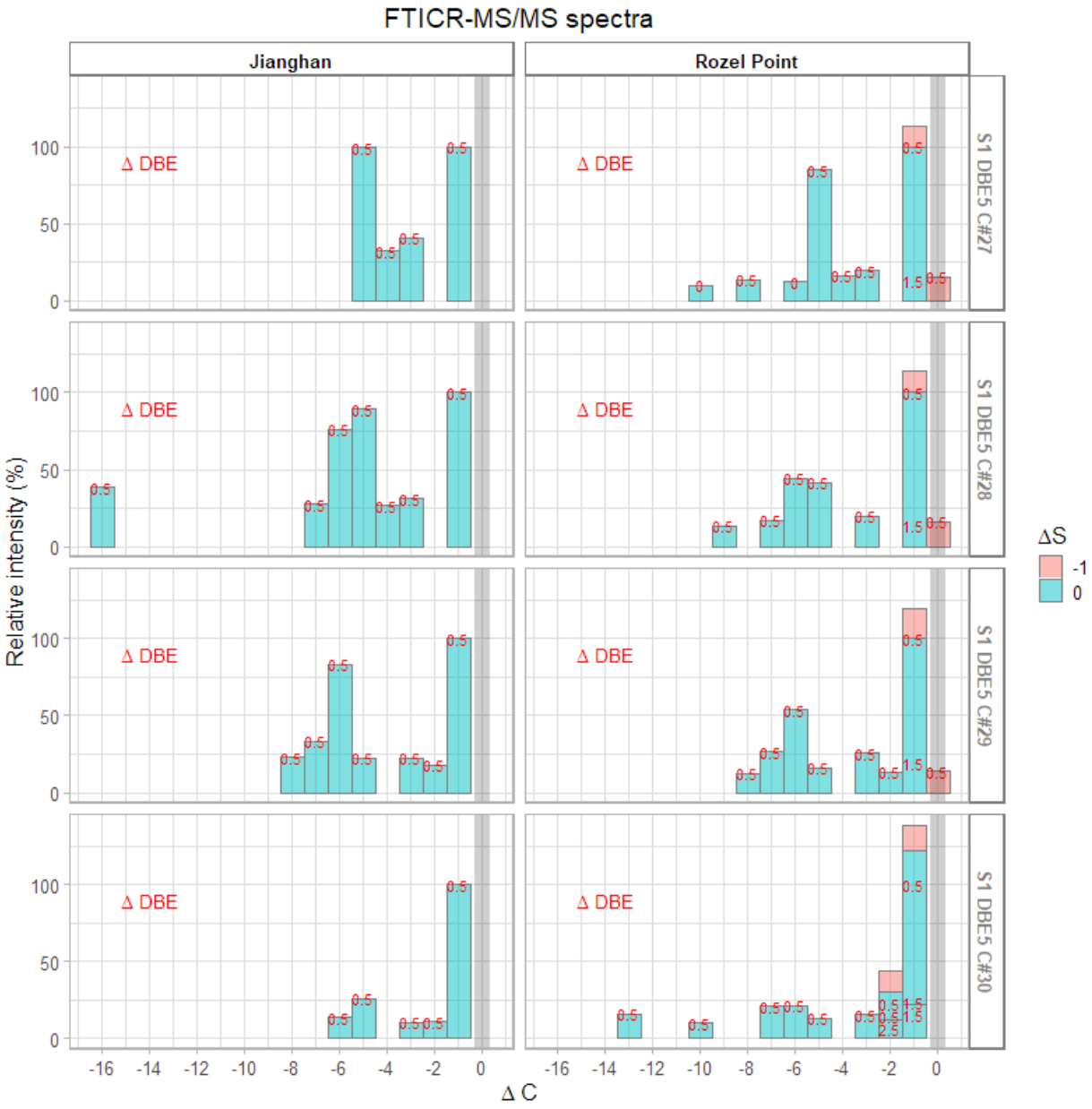

Figure 9. Representation of the APPI-P FTICR-MS/MS spectra of class S_1 DBE 5 C_{27-30} species. Detected fragments are shown as bars based on their compositional differences to the parent peak: carbon number (x-axis), sulfur number (colors) and DBE (labels). Relative intensities are normalized to the most intense daughter ion. The parent peak, represented by a gray bar with arbitrary y-axis values, is not considered in the relative intensity calculations. Fragments with carbon or sulfur number higher than the parent peak, as well as those with relative intensity <10%, are not shown.

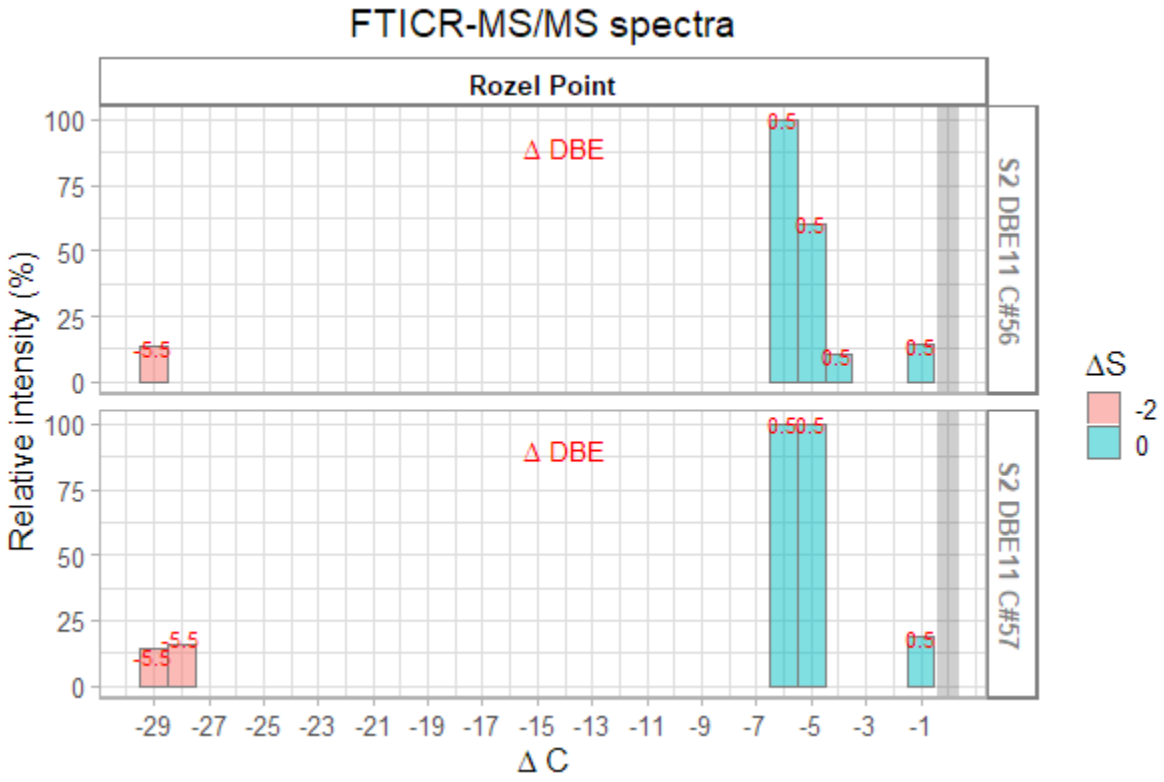

67

68 **Figure 10.** Representation of the Rozel Point oil APPI-P FTICR-MS/MS spectra of class S_2•
69 DBE 11 C_{56-57} species. Detected fragments are shown as bars based on their compositional
70 differences to the parent peak: carbon number (x-axis), sulfur number (colors) and DBE (labels).
71 Relative intensities are normalized to the most intense daughter ion. The parent peak, represented
72 by a gray bar with arbitrary y-axis values, is not considered in the relative intensity calculations.
73 Fragments with carbon or sulfur number higher than the parent peak, as well as those with
74 relative intensity <10%, are not shown.

75
76

Table 1. Sample codes and geochemical overview.

Code	Oil	Location	Sulfur (wt %)	Organic matter source	Depositional environment	Thermal maturity	Biodegradation	References
RP	Rozel Point	Utah, USA	9.4	Marine - lacustrine	hypersaline, lacustrine	Immature	Moderate	(Meissner et al., 1984; ten Haven et al., 1988; Sinninghe Damsté et al., 1989)
JH	Jianghan	Eastern China	5.6	Marine - lacustrine, with terrigenous inputs	hypersaline, lacustrine	Immature	Moderate	(Philp and Zhaoan, 1987; Carroll and Bohacs, 2001; Hou et al., 2017)
GR	Peace River	NW- Central Alberta, Canada	5.5	Marine - lacustrine, with terrigenous inputs	Marine - lacustrine	Mature - overmature	High	(Riediger, 1994; Adams et al., 2012; Adams et al., 2013; Bennett et al., 2013)
BS	Peace River	NW- Central Alberta, Canada	4.1	Marine - lacustrine	Marine - lacustrine	Mature - overmature	Very High	
WC	Peace River	NW- Central Alberta, Canada	4.2	Marine - lacustrine	Marine - lacustrine	Mature - overmature	High	